PFC/JA-83-13

PARAMETRIC PHENOMENA IN ELECTRON CYCLOTRON RESONANCE HEATING OF TOKAMAK PLASMAS

V. Stefan* and A. Bers

March 1983

*Permanent address: "Boris Kidrič" Institute of Nuclear Sciences, Vinča, Beograd, Yugoslavia.

Parametric Phenomena in Electron Cyclotron Resonance Heating of Tokamak Plasmas†

V. Stefan* and A. Bers

Plasma Fusion Center
Massachusetts Institute of Technology
Cambridge, Massachusetts 02139, U.S.A

Abstract

A theoretical study of parametric processes near the electron cyclotron resonance region in tokamak plasmas is presented. Parametric dispersion relations, including finite wave length of the driver pump, of principal and harmonic parametric excitations, are given. The problem of primary and secondary decays including their temporal and spatial growth rates is studied. In the nonlinear phase of development of the excited waves, a cascading saturation mechanism is invoked for both convective and absolute instabilities. Anomalous absorption frequencies and anomalous absorption lengths are evaluated for a variety of parametric excitations. Finally, a comparison between linear and nonlinear absorption processes is given.

† Work supported by DOE Contract No. DE-AC02-78ET-51013.

* Permanent address: "Boris Kidrič" Institute of Nuclear Sciences, Vinča, Beograd, Yugoslavia.

1. Introduction

The excitation of intense high-frequency plasma waves represents a promising method for additional heating of tokamak plasmas. In the lower-hybrid frequency range (LHFR)[1] linear and nonlinear theory of plasma heating is relatively well developed[2]. The recent development of gyrotrons (electron-cyclotron masers)[3] has made it possible to carry out electron cyclotron resonance heating (ECRH) in tokamaks[4]. Interaction of high-frequency electromagnetic radiation with plasmas at ECR could be also used as a prime plasma production technique[5]. Up-to-date papers on plasma heating in this frequency range have mainly dealt with linear theory[6] (and references therein) while only a few papers[7−9,36] considered nonlinear interactions of a driver pump with plasmas.

In papers dealing with linear electron-cyclotron resonance heating (LECRH) it was shown that both ordinary (O) and extraordinary (X) electromagnetic waves (Figures 1 and 2) could be used for plasma heating if they are launched from the appropriate (high or low field) side of the tokamak and at appropriate angles to a toroidal magnetic field $\vec{B}_T$. In open systems (mirror-confined plasmas)[10], without plasma preheating by other means, if $\Omega_e > \omega_{pe}$ (Ω_e-electron cyclotron frequency and ω_{pe} electron plasma frequency) the main part of the energy is transfered to resonant electrons which are accelerated up to relativistic velocities. In the case of tokamak plasma, which is ohmically preheated, and if $\Omega_e > \omega_{pe}$, bulk plasma heating at ECR is dominant[4]. Linear electron cyclotron resonance heating of high density tokamak plasmas ($\Omega_e < \omega_{pe}$ everywhere in the tokamak) is considered in Ref. 11; propagation of the X-mode launched quasi-perpendicularly in reference to $\vec{B}_T$ from the inside (high-field side) of the torus, and propagation of O-mode launched obliquely to $\vec{B}_T$ from the outside (low-field side) of the torus was considered. It was shown that, finally, in both cases linear conversion into electron Bernstein modes and corresponding cyclotron damping takes place.

The electric field intensities of contemporary gyrotrons are sufficient for appearance of parametric processes in tokamak plasmas.[31] Consequently, nonlinear processes in plasma heating at ECR could play a significant role. The very first experimental investigation of parametric processes at ECFR is given in Ref. 12.

Understanding of parametric excitations in a plasma driven with external e.m. power in the ECFR is important not only for heating but also because it presents a possibility of finding new means for probing and controlling of the plasma density and current profiles. In addition parametric processes can as well significantly change conditions in the domain of linear resonance.

Section 2 discusses, briefly, the linear propagation characteristics of ECFR waves in a tokamak-type plasma. Parametric excitations and their thresholds are described in section 3, and the secondary decay processes are outlined in section 4. Section 5 gives the nonlinearly absorbed energy through cascade saturation and summarizes the anomalous frequencies and absorption lengths for the various parametric excitations. Section 6 outlines some of the limitations of the cascade saturation mechanism, and section 7 compares the linear and nonlinear absorption processes.

2. Accessibility of a Driver Pump at ECFR

Here, we give a brief presentation of accessibility theory at ECFR from the aspect of nonlinear interaction of a driver pump with the plasma. It has already been mentioned that both O and X-mode driver pumps are in use in contemporary experiments for linear heating of tokamak plasmas. The O-mode has an advantage with respect to the X-mode due to its accessibility from both sides (inside and outside) of the tokamak (Figure 3). However, the X-mode is more heavily damped than the ordinary one at oblique incidence from the high-field side[14]. Launched from the low-field side the X-mode reaches the cut-off region defined by $\omega_0 \sim \omega_R$ (Figure 3) where

$$\omega_R(x) = \frac{\Omega_e(x)}{2} + \left[\frac{\Omega_e^2(x)}{4} + \omega_{pe}^2(x)\right]^{1/2} . \qquad (1)$$

This is the so-called right-hand cut-off frequency. The left-hand cut-off frequency is given by the similar expression $\omega_L(x) = -\frac{\Omega_e(x)}{2} + \left[\frac{\Omega_e^2(x)}{4} + \omega_{pe}^2(x)\right]^{1/2}$. (Plasma inhomogeneity gradient is assumed to be along the x-axis.)

Second harmonic heating ($\omega_0 \sim 2\Omega_e(x)$) has also attracted attention [15]. In this case both X and O-mode of the driver pump are accessible from the low-field side. Figures 1 and 2 show propagation characteristics of X and O driver pumps for the case of a strongly magnetized plasma: $\omega_0 \gtrsim \Omega_e \gtrsim \omega_{pe}$.

3. Parametric Coupling at ECFR

In the previous section it was shown that the driver pump, under proper conditions, can reach the center of the tokamak and, consequently, transfer its energy (linearly or nonlinearly) to the dense plasma. Here we shall be interested in parametric excitations of electrostatic (longitudinal) plasma modes in the center of the tokamak. Excitation of electromagnetic modes will not be considered due to their very high group velocity ($\sim c$, the speed of light in vacuum) which leads to relatively high convective threshold fields. In the linear absorption scheme the pump energy is transfered to electrons and if the confinement time is large enough part of this energy could be transferred to ions. In nonlinear (parametric) absorption, however, some of the pump energy can be directly transferred to the ions through the parametrically excited low-frequency plasma modes.

3.1. Mode-Mode Coupling Dispersion Relation

In what follows we shall consider nonlinear interaction of the pump in the form $\vec{E}(t) = \vec{E}_0 \sin(\omega_0 t - \vec{k}_0 \cdot \vec{r})$ with a low β, strongly magnetized plasma ($\Omega_e > \omega_{pe}$). The linear phase of development of parametric instabilities is described by the nonlinear (with respect to the external electric field), resonant, mode-mode coupling dispersion relation obtained through the well-known plasma dielectric permitivity formalism[16],

$$\epsilon^{(0)} + \chi_i^{(0)}\left(1 + \chi_e^{(0)}\right)\left[\frac{e^{(+n)}}{\epsilon^{(+n)}} + \frac{e^{(-n)}}{\epsilon^{(-n)}}\right] = 0 \quad , \quad n = 1, 2\ldots \tag{2}$$

Here $\epsilon^{(0)} = \epsilon(\omega, \vec{k}) \equiv \epsilon_L$ is the low-frequency plasma mode dielectric permitivity; ω and $\vec{k}$ are the frequency and the wave vector of the low-frequency mode; $\epsilon^{(\pm n)} = \epsilon(\omega \pm n\omega_0, \vec{k} \pm n\vec{k}_0) \equiv \epsilon_H$ is the high-frequency magnetized plasma mode dielectric

permitivity; $\omega \pm n\omega_0$, $\vec{k} \pm n\vec{k}_0$ are the frequencies and the wave vectors of the side-bands (Stokes and anti-Stokes); $\chi_i^{(0)} \equiv \chi_i(\omega, \vec{k})$ and $\chi_e^{(0)} \equiv \chi_e(\omega, \vec{k})$ are the low-frequency ion and electron plasma susceptibilities, respectively. The coefficients $e^{(\pm n)}$ describe the couplings of the upper and lower side-bands with the low-frequency plasma mode through the pump electric field. The coupling coefficients, maximized with the following selection rules: $n\omega_0(\vec{k}_0) \approx \omega_H(\vec{k}_H) + \omega(\vec{k})$ and $n\vec{k}_0 \approx \vec{k}_H + \vec{k}$ ($\omega_H \equiv \omega \pm n\omega_0$ and $\vec{k}_H \equiv \vec{k} \pm n\vec{k}_0$), are given by:

$$e_{\max}^{(\pm n)} = \frac{|(\vec{k} \pm n\vec{k}_0)\vec{r}_{EB}|^{2n}}{|\vec{k} \pm n\vec{k}_0|^{2n}} \frac{k^{2n}}{(n!)^2 4^n} \tag{3}$$

where ω_0 and $\vec{k}_0$ are the angular frequency and the wave vector of the pump; and $\vec{r}_{EB}$ is the vector of electron oscilation amplitude in the electric field of the pump and confining (toroidal) magnetic field $\vec{B}_T$. It is given by:

$$\vec{r}_{EB} = \begin{vmatrix} \frac{\omega_0^2}{\omega_0^2 - \Omega_e^2} & \frac{-i\omega_0\Omega_e}{\omega_0^2 - \Omega_e^2} & 0 \\ \frac{i\omega_0\Omega_e}{\omega_0^2 - \Omega_e^2} & \frac{\omega_0^2}{\omega_0^2 - \Omega_e^2} & 0 \\ 0 & 0 & 1 \end{vmatrix} \frac{e\vec{E}_0}{m_e\omega_0^2} \tag{4}$$

In (4) E_0 is the complex electric field amplitude of the pump in vacuum, and e and m_e the charge and mass of electrons, respectively.

It is to be noted that relation (2) describes parametric decay processes as well as oscillating two-stream instabilities (OTSI) in magnetized plasma. In what follows, however, we shall mainly deal with decay processes at ECFR while the significance of the OTSI will be only qualitatively described.

In the case of parametric decay processes [$e^{(+n)}$ is then neglected in (2)] the parametric dispersion relation (2) predicts the excitation of a high-frequency mode with frequency ω_H and low-frequency mode with frequency $\omega = \omega_L - \vec{k}_0 \cdot \vec{V}_H$ where ω_L is the low plasma eigen-frequency and $\vec{V}_H = -(\partial \operatorname{Re} \epsilon_H / \partial \vec{k}_H)/(\partial \operatorname{Re} \epsilon_H / \partial \omega_H)$ is the group velocity of the high frequency mode. In what follows, however, this finite wavelength low-frequency shift will not play a significant role because we shall be interested in the excitation of high-frequency magnetized plasma modes with $\vec{V}_H \perp \vec{k}_0$. From (2) the parametric decay growth rate $\gamma \equiv \gamma_d$, for weakly damped waves, is found to be:

$$\gamma_d^2 = \left\{\left[e^{(-n)}\right] - \left[e_{THR}^{(-n)}\right]\right\}[1 + \mathrm{Re}\,\chi_e(\omega,\vec{k})]^2\left(\frac{\partial\,\mathrm{Re}\,\epsilon_L}{\partial\omega}\right)^{-1}_{\omega=\omega_L}\left(\frac{\partial\,\mathrm{Re}\,\epsilon_H}{\partial\omega}\right)^{-1}_{\omega=\omega_H} \quad (5)$$

Here $e_{THR}^{(-n)}$, given later in (14), is the threshold value of the coupling coefficient. Expression (5) is obtained under the assumption that $\gamma \gg \gamma_H, \gamma_L$ where γ_H and γ_L are linear damping rates of high and low frequency modes given by: $\gamma_H = -(\mathrm{Im}\,\epsilon_H)/(\partial\,\mathrm{Re}\,\epsilon_H/\partial\omega_H)$, $\gamma_L = -(\mathrm{Im}\,\epsilon_L)/(\partial\,\mathrm{Re}\,\epsilon_L/\partial\omega_L)$.

In this case $e^{(-n)} \gg e_{THR}^{(-n)}$. For $e_{THR}^{(-n)} = 0$, the expression (5) will be referred to as the dissipation free parametric growth rate. For the case $\gamma_H < \gamma < \gamma_L$ the parametric growth rate could be obtained by replacing γ_d^2 in (5) with $\gamma\gamma_L$. This is the case of an isothermal plasmas ($T_e \sim T_i$) typical for tokamaks when the low-frequency plasma mode is heavily damped (quasi-mode) i.e., $\gamma_L \sim \omega_L$.

3.2. Plasma Eigen-modes at ECFR

The spectrum of longitudinal oscillations of a fully ionized (electron-ion) magnetized plasma is described by the following dispersion relation [17] (see also [18]):

$$\begin{aligned}\epsilon(\omega,\vec{k}) &= \mathrm{Re}[\epsilon(\omega,\vec{k})] + i\,\mathrm{Im}[\epsilon(\omega,\vec{k})] \\ &= 1 + \sum_\alpha \frac{1}{k^2 r_{D\alpha}^2}\left\{1 - \sum_{n=-\infty}^{+\infty}\frac{\omega A_n(z_\alpha^2)}{\omega - n\Omega_\alpha} J_+(\beta^{(n)}\alpha)\right\} + i\epsilon_{coll} = 0\end{aligned} \quad (6)$$

Here $A_n(z_\alpha^2) = \exp(-z_\alpha^2) I_n(z_\alpha^2)$ where I_n is the modified Bessel function of order "n", $z_\alpha^2 = \frac{k_\perp^2 \Omega_\alpha^2}{v_{T\alpha}^2}$ and $\beta_\alpha^{(n)} = \frac{\omega - n\Omega_\alpha}{|k_z| v_{T\alpha}}$ ($v_{T\alpha}$ is the thermal velocity of "α" species of particles). The function $J_+(\beta)$ is defined as:

$$J_+(\beta) = \beta\exp(-\frac{\beta^2}{2})\int_0^\beta \exp(\frac{x^2}{2})dx - i\sqrt{\frac{\pi}{2}}\beta\exp(-\frac{\beta^2}{2}) \quad (7)$$

For the high-frequency dielectric permittivity in the long-wave-length region ($k^2\rho_e^2 \ll 1$, $k^2 r_{De}^2 \ll 1$, ρ_e the electron Larmor radius, r_{De} the electron Debye radius) we obtain from (6) the following dispersion relation

$$\epsilon_H(\omega,\vec{k}) = 1 - \frac{\omega_{pi}^2\cos^2\theta}{\omega^2} - \frac{\omega_{pi}^2\sin^2\theta}{\omega^2 - \Omega_i^2} - \frac{\omega_{pe}^2\cos^2\theta}{\omega^2} - \frac{\omega_{pe}^2\sin^2\theta}{\omega^2 - \Omega_e^2} + i\epsilon_{coll}\,. \quad (8)$$

The collisional dissipation of magnetized plasma eigen-modes is given by:

$$\epsilon_{coll} = \frac{\omega_{pe}^2 \nu_{ei}}{\omega^3}\left[cos^2\theta + \sin^2\theta \frac{\omega^2(\omega^2+\Omega_e^2)}{(\omega^2-\Omega_e^2)^2}\right]. \tag{9}$$

If $\Omega_e \gtrsim \omega_{pe}$ we obtain the following cold magnetized plasma modes:

$$\omega_H \sim \left\{\Omega_e(1+\frac{\omega_{pe}^2}{2\Omega_e^2}\sin^2\theta)\,;\ \omega_{pe}|\cos\theta|\right\} \equiv \omega_{\pm}\,. \tag{10}$$

Parametric excitation of eigen-mode $\omega_- = \omega_{pe}|\cos\theta|$ (Gould-Trivelpiece (GT) mode or oblique Langmuir wave) and the corresponding heating of the plasma by this wave was already considered in Ref. 7, 8, and 19 and will be excluded here. It must be noted, however, that in the case of tokamak plasmas ($\omega_{pe} > \Omega_e$) the frequency curves $\omega_{UH}(x)$, $\Omega_e(x)$ and $\omega_{pe}(x)$ (Figure 3a) are overlapped and consequently the shaded area on tokamak cross section (Figure 3b) presents the region where simultaneous parametric excitation of upper-hybrid wave (UH), electron cyclotron wave (EC) and G-T modes occur.

In the case of nearly perpendicular propagation, ω_+ is reduced to the upper-hybrid mode $\omega_{UH}^2 = \omega_{pe}^2 + \Omega_e^2$. Perpendicular propagation in this frequency region also involves electron Bernstein modes with a frequency spectrum given, approximately, by

$$\omega_{EB} \sim n|\Omega_e|\left\{1+\frac{I_n(k^2\rho_e^2)}{k^2 r_{De}^2}e^{-k^2\rho_e^2}\right\}, \tag{11}$$

and corresponding dielectric permittivity

$$\epsilon_{EB}(\omega,\bar{k}) = 1 - \frac{\omega_{pe}^2}{\omega}\sum_{n=-\infty}^{+\infty}\frac{n^2 A_n(k^2\rho_e^2)}{k^2\rho_e^2(\omega-n\Omega_e)} + in!2^n\frac{k^2 r_{DE}^2}{(k^2\rho_e^2)^n}\frac{\nu_{ei}}{n|\Omega_e|}\,. \tag{12}$$

where the last term, due to collisions, is evaluated for $k^2\rho_e^2 < 1$,

It is evident from (11) that electron Bernstein modes in the long-wave length region ($k^2\rho_e^2 \ll 1$) and for $n = 1$ reduces to the upper hybrid mode.

In the case of dense plasmas ($\omega_{pe} > \Omega_e$) we have:

$$\omega_H \sim \left\{\omega_{pe}(1+\frac{\Omega_e^2}{2\omega_{pe}^2}\sin^2\theta)\,;\ \Omega_e|\cos\theta|\right\}. \tag{13}$$

The first mode is not of interest because $\omega_H \sim \omega_{pe}$ and the second mode has the frequency equal to the local electron cyclotron frequency $\Omega_e(x)$ only in the case of longitudinal propagation.

In the low-frequency domain there exist high-frequency ion-sound waves $IS(H)$ ($\omega_L = kV_s$, $V_s = (\frac{Te}{mi})^{1/2}$), low-frequency ion-sound wave $IS(L)$ ($\omega_L = kV_s \cos\theta$), ion-Bernstein modes (IB) $\left(\omega_L = m|\Omega_i|\left\{1 + \frac{I_m(k^2\rho_i^2)}{k^2 r_{Di}^2} e^{-k^2\rho_i^2}\right\}\right)$ and lower hybrid wave $LH\left(\omega_L \sim \omega_{pi}\left(1 + \frac{\omega_{pe}^2}{\Omega_e^2}\right)^{-1/2}\right)$.

In what follows we shall be interested in excitation of modes with frequencies equal to the local electron cyclotron frequency coupled to the above listed low-frequency modes.

3.3. Threshold Value Problem at ECFR

From the parametric dispersion relation (2), the threshold value for decay processes is found to be:

$$\left\{e_{THR}^{(-n)}\right\} = \gamma_H \gamma_L \frac{1}{[1 + \mathrm{Re}\,\chi_e(\omega, \vec{k})]^2} \left(\frac{\partial \epsilon_H}{\partial \omega}\right)_{\omega=\omega_H} \left(\frac{\partial \epsilon_L}{\partial \omega}\right)_{\omega=\omega_L} \tag{14}$$

This expression gives us the so-called dissipative threshold of convective parametric instabilities in homogeneous magnetized plasmas. The threshold values for absolute parametric instabilities are higher and are given by [Ref. 20]

$$\gamma_{do} = [\gamma_H |V_L| + \gamma_L |V_H|]/2\sqrt{|V_H||V_L|} \equiv \gamma_a \tag{15}$$

where γ_{do} is γ_d of (5) with $e_{THR} = 0$. Here V_H and V_L are group velocities of high and low-frequency parametrically excited modes.

Taking into account inhomogeneity of plasma, the conditions that the linear instabilities evolve to large amplitudes are Ref. 21

$$\gamma_{do} \gg (2\gamma_a/\pi) \quad \text{and} \quad (\pi\lambda) \gg 1 \tag{16a}$$

for initially evolving absolute instabilities, and

$$\gamma_{do} \gg 2(\gamma_1 + \gamma_2)/\pi \quad \text{and} \quad (\pi\lambda) \gg 1 \tag{16b}$$

for initially convective instabilities. Here $\lambda \equiv \gamma_{do}^2/\kappa'|V_H V_L|$ where $\kappa' = (d/dx)[k_0(x) - k_H(x) - k_L(x)]$.

From (14) it is evident that threshold values of the pump field depend on linear disspation processes of the parametrically excited modes. (See Table I.) In what follows we shall be interested in bulk plasma heating which is realized through collisional dissipation of high-frequency modes. On the other hand if the dissipation of high-frequency modes is noncollisional (Landau or electron-cyclotron damping) the threshold value increases exponentially. If the decay wave number k_d satisfies the following condition: $k_d \ll k_{coll}$, where

$$k_{coll}^2 r_{De}^2 \sim \frac{\Omega_e^2}{\omega_0^2 - \omega_{pe}^2 - \Omega_e^2} \left\{ \ln \left(\frac{\omega_0}{\nu_{ei}} \right)^2 \right\}^{-1}, \tag{17}$$

dissipation of high-frequency modes is dominantly collisional. In Table I we give the linear damping rates of the parametrically excited modes in ECFR.

From (14) and (3) ($k_0 \sim 0$ in the case of primary excitations) for principal harmonic excitations ($n = 1$) and for tokamak parameters $n_e \sim 10^{12}\, cm^{-3}$, $T_e \sim 200\, eV - 1\, keV$, $f_0 = (\omega_0/2\pi) \gtrsim [\Omega_e(R_o)]/[2\pi] = 10 - 40\, GHz$ one finds threshold electric fields in the range $E_0 \sim 30 - 120\, V/cm$ (for parametric channels given in Table III). The corresponding power flux is $I_{0,thr} = 2 - 50\, W/cm^2$ and, if the area of electron resonance is $S \sim 100\, cm^2$, the threshold power is $P_o = 200 - 5 \cdot 10^3\, W$. The threshold values taking into account plasma inhomogeneity ($\pi\lambda = 1$, see Eq. 16) can be obtained from (14) by substituting γ_H and γ_L with V_H/L and V_L/L, respectively, where $L = [\pi/(\kappa')_{x=R_0}]^{1/2}$. Convective threshold due to the plasma inhomogeneity is enhanced approximately by an order of magnitude so that $E_{0,thr} \gtrsim 1\, (kV/cm)$, $I_{0,thr} \gtrsim 1\, (kW/cm^2)$ and $P_{0,thr} > 100\, kW$, which is available in current experiments on tokamaks with parameters in the above range (Versator II, FT-1, ISX-B, PLT, T-10 and JFT-2). For detailed threshold value analyses see Refs. 7, 8 and 36.

In the case of high-density and high magnetic field tokamaks with parameters in the range $n_e \sim 10^{14}\, cm^{-3}$, $f_0 \sim 100 - 200\, GHz$, and $T_e \gtrsim 1\, keV$ (like Alcator C and T-15) the threshold power flux is $P_{0,thr} \gg 10 kW/cm^2$. In current experiments

the maximum power flux available is around $10kW/cm^2$. Consequently significant parametric processes at ECR are not to be expected for these tokamaks until the power flux is raised up by an order of magnitude.

4. Secondary Decay Processes

As the saturation mechanism of the parametrically induced turbulent plasma state, secondary decays of high-frequency magnetized plasma modes $\omega_{H_1}(\vec{k}_{H_1})$ into other high-frequency $\omega_{H_2}(\vec{k}_{H_2})$ modes coupled with low-frequency modes $\omega_{L_2}(\vec{k}_{L_2})$, etc. are considered. This mechanism, as it will be shown later, yields a high absorption efficiency. In the lower hybrid frequency range (LHFR) it was used in Ref. 19 and in explanation of space simulation experiments in Ref. 22. In the case of secondary decay processes the finite wave length of the driver pump (high-frequency longitudinal mode) must be taken into account in contrast to the case of primary decays where the dipole approximation ($k_0 = 0$) is valid. The parametric mode-mode coupling dispersion relation describing secondary decay processes has the following form (2) (principal harmonic excitation $n = 1$).

$$\epsilon(\omega^L_{n+1},\vec{k}^L_{n+1})\epsilon(\omega^L_{n+1}-\omega^H_n,\vec{k}^L_{n+1}-\vec{k}^H_u)+ \\ +\frac{k^2_{n+1}}{4}\frac{[(\vec{k}^L_{n+1}-\vec{k}^H_n)r^{(n)}_{EB}]^2}{(\vec{k}^L_{n+1}-\vec{k}^H_n)^2}\chi_i(\omega^L_{n+1},\vec{k}^L_{n+1})\Big[1+\chi_e(\omega^L_{n+1},\vec{k}^L_{n+1})\Big]=0\,. \tag{18}$$

Here $(\omega_n, \vec{k}_n)$ are the frequency and the wave vector of the n-th cascade, and $r^{(n)}_{EB}$ is oscillation amplitude of electrons in the high-frequency electric field of n-th cascade. [See (4).]

4.1. Absolute Secondary Decay Instabilities

From (18), the parametric growth rate of the n-th cascade is found to be:

$$\gamma^2_n=\frac{k^2_{n+1}}{4}\frac{[(\vec{k}_{n+1}-\vec{k}_n)\vec{r}_{EB}]^2}{(\vec{k}_{n+1}-\vec{k}_n)^2}[1+\mathrm{Re}\,\chi_e(\omega_{n+1},\vec{k}_{n+1})]^2\Big(\frac{\partial\,\mathrm{Re}\,\epsilon_L}{\partial\omega}\Big)^{-1}_{\omega=\omega_L}\Big(\frac{\partial\,\mathrm{Re}\,\epsilon_H}{\partial\omega}\Big)^{-1}_{\omega=\omega_H} \tag{19}$$

Here $\omega_H \equiv \omega_H(\vec{k}_n^H - \vec{k}_{n+1}^L)$ and $\omega_L \equiv \omega_L(\vec{k}_{n+1}^L)$. Expression (19) is obtained under the assumption that $\gamma_n > \gamma_n^H, \gamma_n^L$ where γ_n is the temporal growth rate of the secondary decay instabilities. In the model of a homogeneous plasma, if $V_H V_L < 0$ the parametric decay instabilities are absolute if[20,23] [see (15)],

$$\frac{1}{2}\gamma_L\left(\frac{V^H}{V^L}\right)^{1/2} < \gamma_n < \omega_L \tag{20}$$

In (20) the demand for the discrete (line-like) turbulence spectrum ($\gamma_n < \omega_L$) is also taken into account. Due to the inhomogeneity of tokamak plasmas and for weaker driver pumps, parametrically excited high-frequency instabilities could become convective and, consequently, the instability description by a temporal growth rate is not adequate.

4.2. Convective Secondary Decay Instabilities

If $V_H V_L > 0$ the energy of excited waves is effectively convected away from the region of primary excitation. Consequently, processes in that region may be linear with respect to electric field amplitudes of excited waves. However on the length $\ell \sim 1/(\mathrm{Im}\, k_H)$ amplification of high-frequency mode electric field could be significant and nonlinear dissipation of the modes dominant. The maximum spatial growth rate is:

$$(\mathrm{Im}\, k_H)^2 = \frac{\gamma_d^2}{|V_L V_H|} \tag{21}$$

Here γ_d is the dissipation-free temporal growth rate and V_H and V_L group velocities evaluated at $\vec{k} = \vec{k}_0 - \vec{k}_d$ and $\vec{k} = \vec{k}_d$, respectively; k_d is decay wave number defining the location of primary decays in $\vec{k}$-space. In Table II the values of k_d for primary decays of interest are given.

The expression (21) is valid if the excited modes are weakly damped, i.e. $\gamma > \gamma_L, \gamma_H$. In the case of excitation of low-frequency quasi-modes (LFQM) the inequality $\gamma_H < \gamma < \gamma_L$ is satisfied. Then:

$$\mathrm{Im}\, k_H = \frac{\gamma_d}{|V_H|} \tag{22}$$

Note that in the case of very high group velocities of high-frequency modes amplification occurs on a large distance which could be larger than the dimensions of interaction region[20,24] or even than the (radial) dimensions of the tokamak plasma. In that case nonlinear dissipation of excited waves does not play any significant role. However, we shall be interested in relatively slow waves, longitudinal waves, and their saturation distance ℓ_a (ℓ_a is the anomalous absorption length to be defined in 5.3).

5. Nonlinearly Absorbed Energy

In the model of cascade saturation the nonlinearly absorbed energy is given by:

$$Q^{ABS} = 2\gamma_0(E_0)W_1 \tag{23}$$

in the case of absolute instabilities, or by

$$Q^{CONV} = 2\,\mathrm{Im}[k_0(E_0)]V_H W_1 \tag{24}$$

in the case of convective instabilities. Here $\gamma_0(E_0)$ and $\mathrm{Im}[k_0(E_0)]$ are primary temporal and spatial growth rates, respectively. $W_1(\omega_1, k_1^H)$ represents the energy contained in the first cascade of the high-frequency mode and is given by [Ref. 25]

$$W_1(\omega_1, k_1^H) = \left\{\frac{\partial}{\partial\omega}[\omega\,\mathrm{Re}\,\epsilon^H(\omega,\vec{k})]\right\}_{\omega=\omega_1(\vec{k}_1^H)} \frac{|\vec{E}(\vec{k}_1^H,\omega_1)|^2}{8\pi} \tag{25}$$

In order to find Q, as it is evident from (23) and (24), we must know the turbulence spectrum $W_n(\vec{k},\omega)$ and particularly $W_1(\vec{k}_1^H,\omega_1)$. The answer could be obtained from the turbulence theory based on cascading saturation mechanism. A complete development of turbulence theory based on nonlinear kinetic equations in LHFR is given in Ref. 19. Here, however, we shall give a simple power-balance formalism of turbulence processes at ECFR based on the cascade saturation mechanisms.

5.1. Power Balance Theory of Cascading Processes in ECFR

The cascade saturation mechanism was first used in Ref. 26 for studying isothermal plasma and later in Ref. 27 for consideration of nonisothermal plas-

mas. Power balance theory for isotropic plasmas is proposed in Ref. 28 and for anisotropic plasmas in Ref. 9.

We shall consider a quasistationary turbulence spectrum consisting of N cascades with frequency width $\delta\omega \sim \max\{\gamma_n, \gamma_H, \gamma_L\}$. In the weak turbulence theory $\gamma_n \ll \omega_L$ (and $\gamma_L \lesssim \omega_L$) the turbulence spectrum could be considered as discrete, consisting of N discrete lines located at frequency intervals equal to ω_L. In the case $\gamma \lesssim \omega_L$, a ponderomotive force affects the low-frequency mode dispersion features and mode-mode coupling dispersion relation (2) is no longer valid. Consequently a strong coupling of excited waves occurs. For $\gamma \gtrsim \omega_L$ the turbulence spectrum is continuous and power-balance theory is not applicable. For high temperature tokamak plasmas $T_e > 1\ keV$ the inequality $\gamma_H \ll \gamma_L$ is always valid and consequently the turbulent level of low-frequency modes is significantly less in comparison with turbulent level of the high-frequency modes. Accordingly, it could be considered that the low-frequency wave energy is completely dissipated through the linear Landau damping mechanism (or linear cyclotron damping). This becomes more pronounced for isothermal plasmas ($\gamma_s \sim \omega_s \sim kV_{Ti}, V_{Ti} = (Ti/m_i)^{1/2}$) when dispersion relation (2) describes processes of induced scattering of a driver pump (external electric field or longitudinal high-frequency plasma mode) by ions or electrons.

The stationary turbulence spectrum of the high-frequency magnetized plasma modes, in the case of absolute instabilities, is described by

$$\gamma_{n-1}(W_n^H + W_n^L) = \gamma_H W_n^H + \gamma_L W_n^L + \gamma_n(W_{n+1}^H + W_{n+1}^L)\,,\ n \geq 1\,. \qquad (26)$$

Here $\gamma_{n-1}(W_n^H + W_n^L)$ represents the power contained in the n-th cascade which is partly linearly dissipated collisionally in high-frequency mode $\gamma_H W_n^H$ and noncollisionally in low-frequency mode $\gamma_L W_n^L$. The flow of energy into $(n+1)$-th high and low-frequency cascade is accounted for by $\gamma_n(W_{n+1}^H + W_{n+1}^L)$. It must be noted that taking into account finite wave length of the driver pump ($\vec{k}_0 \neq 0$) leads to the appearance of the "blue" lines (with frequencies higher than ω_0) in the high-frequency mode turbulence spectrum [Ref. 29]. In Figure 4 the direction of cascading processes for the case of normal and anomalous (points 1,2,4) dispersion

of electron Bernstein modes are shown.

In the case of convective instabilities the energy balance equation takes the following form:

$$\mathrm{Im}\, k_{n-1} V_H (W_n^H + W_n^L) = \gamma_H W_n^H + \gamma_L W_n^L + \mathrm{Im}\, k_n V_H (W_{n+1}^H + W_{n+1}^L), n \geq 1. \quad (27)$$

Correlation between the energy content in low and high-frequency parametrically excited modes is given by:

$$W_n^L = (N - n + 1) \frac{\gamma_H}{\gamma_L} \frac{\omega_L}{\omega_H} W_n^H \ , \ n = 1 \ldots N \quad (28)$$

It is evident from (28) that W_n^L could be neglected in (26) and (27). In (28) N is the total number of cascades. Substituting the expression for parametric temporal growth rate (5) into (26), or spatial growth rates (21), (22) into (27), a turbulence spectrum of high-frequency modes could be obtained. In the case of convective instabilities we have:

$$E_n = \frac{\gamma_H}{\mathrm{Im}\, k_0 (V_L V_H)^{1/2}} E_0 \left(\frac{\mathrm{Im}\, k_0 (V_L V_H)^{1/2}}{\gamma_H} - \frac{n}{3} \right); \quad n = 0 \ldots N \quad (29)$$

In (29) $\gamma_n > \gamma_H, \gamma_L$ is assumed. E_n is the electric field amplitude of n-th cascade and E_0 is the free-space electric field amplitude of the driver pump. From (29) with $(E_N = E_{thr} \ , \ E_0 \gg E_{thr})$ we obtain for the total number of cascades,

$$N \sim 3 \frac{\mathrm{Im}\, k_0 (|V_H V_L|)^{1/2}}{\gamma_H} \ . \quad (30)$$

Putting $n = 1$ in (29) we obtain:

$$E_1 \sim E_0 \ . \quad (31)$$

This result is, however, only valid in the case when primary growth rate $\gamma_0(E_0)$ is of the same nature as the secondary one $\gamma_1(E_1)$. (This was assumed in obtaining (29).) The more general case is when the primary parametric growth rate is not of the same nature as the secondary one; for example when an e.m. wave decays into high and low-frequency longitudinal modes and the high-frequency mode decays, further, into two high-frequency modes; this is possible in the short wave length

region ($k\rho_e \gg 1$) of second harmonic electron Bernstein mode ($2\Omega_e \rightarrow \Omega_e + \Omega_e$). In this paper such secondary decays will not be treated.

Equation (26) (for $n = 1$) could be solved by means of the approximation $W_1 \sim W_2$ (the error is minimum $\Delta = W_1 - W_2$, $W_1 = W_n + (n-1)\Delta$). Then $\gamma_0(E_0) \sim \gamma_1(E_1)$ is obtained. From this equation for E_1

$$E_1 = f(E_0) \tag{32}$$

could be obtained. Note that (32) is obtained under the assumption of negligible linear dissipation of the high-frequency cascades ($\gamma_0 \gg \gamma_H$) for the case of absolute instabilities (Eq. 26), and in the case of convective instabilities (Eq. 27) under the assumption that $1/(\mathrm{Im}\, k_1^H) \ll V_H/\gamma_H$, i.e., that the amplification length of the primary excited high-frequency mode is less than its linear damping length. This is realized if the driver pump electric field is strong enough.

For the absorbed energy, from (32) and (23), we obtain

$$Q^{ABS} = 2\gamma_1(E_1)\frac{(f(E_0))^2}{4\pi} \tag{33}$$

From (33) we see how the secondary decay processes play a determining role in the energy absorption. In what follows we shall be interested in the cases when primary and secondary decays are of the same nature, so that

$$Q^{ABS} = 2\gamma_1(E_1)\frac{E_0^2}{4\pi} \tag{34}$$

If the low-frequency modes are weakly damped ($\gamma > \gamma_L$), we obtain from (23), (24) and (21)

$$Q^{CONV} = \left(\frac{V_H}{V_L}\right)^{1/2} Q^{ABS} \quad , \quad \gamma > \gamma_H, \gamma_L \,. \tag{35}$$

In the case of heavily damped low-frequency modes (quasi-modes) the corresponding relation could be obtained from (23), (24) and (22)

$$Q^{CONV} = \left(\frac{\gamma_L}{\gamma}\right)^{1/2} Q^{ABS} \quad , \quad \gamma_H < \gamma < \gamma_L \,. \tag{36}$$

The expressions (33) – (36) give the relation between the energies nonlinearly absorbed (through cascading processes) by convective and absolute instabilities. (The problem of determining when particular parametric instabilities are convective or absolute is out of the scope of this paper; see for example Ref. 30). In the case of laser-plasma interactions convective instabilities (due to the inhomogeneity of plasma) always enhances [see (35)] the absorption with respect to the absolute instability. In ECFR in the case of "cold" modes:

$$\omega^{uh} = \omega_{UH}\left\{1 - \frac{1}{2}\frac{\omega_{pe}^2\Omega_e^2}{\omega_{uh}^4}\frac{k_\parallel^2}{k^2}\right\}, \tag{37}$$

where $\omega_{uh}^2 = \omega_{pe}^2 + \Omega_e^2$, and

$$\omega^{LH} = \omega_{lh}\left(1 + \frac{m_i}{m_e}\frac{k_\parallel^2}{k^2}\right)^{1/2} \tag{38}$$

where $\omega_{lh} = \left[\omega_{pi}/(1 + \frac{\omega_{pe}^2}{\Omega_e^2})^{1/2}\right]$ For these modes $V^{UH}/V^{LH} \sim (m_e/m_i)^{1/2}(\omega_{pe}/\Omega_e) \ll 1$ is obtained. If "hot" modes are excited:

$$\omega^{UH} = \omega_{uh}\left\{1 - \frac{1}{2}\frac{\omega_{pe}^2}{\omega_{uh}^2}k_\perp^2\rho_e^2\right\} \tag{39}$$

$$\omega^{LH} = \omega_{lh}\left\{1 + \frac{3}{2}k_\perp^2\rho_e^2\frac{\Omega_e\Omega_i}{\omega_{pi}^2}\frac{T_i}{T_e}\right\} \tag{40}$$

the group velocities ratio is $(V^{UH}/V^{LH}) \sim (V^{EB}/V^{LH}) \sim (1/3)(\omega_{pe}/\Omega_e)^2(\omega_{pi}/\Omega_i)(T_e/T_i) > 1, (\omega_{pi} \gg \Omega_i)$. Hence in the case of excitation of "hot" modes (convectively unstable) the nonlinear absorbtion of energy is enhanced.

5.2. Anomalous Absorption Frequency

In the cascade saturation mechanism energy transferred from the external pump into the first cascade is collisionally dissipated through N further cascades. The condition for collisional dissipation of the high-frequency mode (in a high-temperature plasma it is a weak linear dissipation) is essential because only in this

case is a significant turbulence level of high-frequency modes achieved. In such a situation the nonlinear dissipation of parametrically excited high-frequency modes is dominant. The opposite case is encountered with low-frequency modes where a strong linear dissipation is assumed (linear Landau damping or cyclotron damping); in this case the appearance of low-frequency parametric turbulence is excluded.

Based on the law of conservation of energy we can write:

$$\nu_a W_0 = 2\gamma_0(E_0)W_1 = 2\sum_{n=1}^{n=N} \gamma_H W_n \quad ; \quad \gamma_H \sim \nu_{ei}\,. \tag{41}$$

The expresion (41) is to be considered as definition of anomalous absorption (collision) frequency. As $W_n \sim W_{n+1}$, $n > 0$ (as a rule in this saturation mechanism), then $\gamma_1(E_1) \sim \gamma_0(E_0)$ which, if the primary and secondary decays are of the same nature, gives (with $W_1 \lesssim W_0$):

$$\nu_a \sim 2\gamma_1(E_1) \sim 2\gamma_0(E_0)\,. \tag{42}$$

From (42) it is evident that the anomalous absorption frequency exceeds the electron-ion collision frequency by a factor of $2[\gamma_0(E_0)]/\nu_{ei}$. In the case of excitation of low-frequency quasi-modes ($T_e \sim T_i$, typical for tokamak plasmas) the anomalous absorption frequency has a quadratic dependence on the external electric field $\nu_a \sim E_0^2$ (see (2) and (3) for $n = 1$).

5.3. Anomalous Absorption Length

The anomalous absorption frequency is to be taken as a local characteristic of nonlinear absorption processes. A high anomalous absorption frequency, however, does not mean, in general, a high nonlinear absorption efficiency. For this reason we shall define another characteristic quantity, namely, the anomalous absorption length as a distance (ℓ_a) which is traversed by the external driver pump with group velocity V_{gr} in the time of nonlinear absorption $t_{NL} \sim (1/\nu_a)$. Accordingly,

$$\ell_a = V_{gr}\frac{E_0^2}{4\pi Q(E_1^2)}\,. \tag{43}$$

In the ECFR $V_{gr} \sim c$ (c is the speed of light in vacuum). Here, $Q(E_1^2)$ is either (34) or (35) for, respectively, absolute or convective instabilities.

In Table III we give the values of ℓ_a for a variety of parametric excitations in ECFR for the case $\gamma > \gamma_H, \gamma_L$. The corresponding expressions of anomalous absorption lengths for low-frequency quasi-mode excitation (ion-acoustic and lower-hybrid quasi-mode) could be obtained by substitution for ℓ_a: $\left(\frac{c\ell_a}{2k_d v_{Ti}}\right)^{1/2}$, for ion-acoustic quasimode, and $\left(\frac{c\ell_a}{2\omega_{LH}}\right)^{1/2}$ in the case of lower-hybrid quasi-mode excitation.

It must be noted, however, that the influence of real conditions (plasma inhomogeneity, finite extent of driver pump, etc.) are indirectly included in (43) through $Q(E_1^2)$ i.e., through the secondary parametric growth rate. This is only approximate. A more accurate description would have to use an appropriate turbulence theory for an inhomogeneous plasma, including the finite extent of the driver pump.

From Table III, in the case of parametric excitation of electron Bernstein modes coupled with lower hybrid quasi-modes, the anomalous absorption length is found to be ($n = 1$):

$$\ell_a = \frac{1}{\pi}\lambda_0 \frac{\beta}{k^2 r_{De}^2}\left(\frac{B_0}{E_0}\right)^2\left(\frac{\Omega_e}{\omega_{pe}}\right)^2; \quad k_d r_{De} \lesssim 1\,. \tag{44}$$

Here, λ_0 denotes the free-space wavelength of the driver pump and $\beta = (8\pi n_e T_e/B_0^2)$ is the "plasma beta". For reactor-type tokamak plasmas with parameters $B_T \equiv B_0 \sim 5 - 10\,T$, $n_e \sim 10^{14}\,cm^{-3}$, $T_e \sim 1 - 5\,keV$, the anomalous absorption length is of the order of $10\,\lambda_0$, if the power flux of the pump is around $100\,kW/cm^2$. For lower density and lower B_0-field tokamak plasmas such an anomalous absorption length can be obtained at significantly lower power fluxes – around $I_0 \lesssim 1\,kW/cm^2$, which is available in current experiments [Ref. 31].

6. Collisional and Noncollisional Nonlinear Dissipation of Parametrically Excited Modes

The cascade saturation mechanism is based on linear collisional dissipation

of high-frequency plasma modes. Consequently, the decay wave number k_d (see Table II) is to be located on the dispersion curve of corresponding parametrically excited modes where collisional dissipation is dominant. On the other hand the decay wave number is a function of "x", (the distance from the tokamak axis), i.e., $k_d = f[\omega_0 - \Omega_e(x)]$ (see Figure 3a and Figure 4), so that as a function of "x", modes with different k_d will be excited. Through cascading processes this mode can enter the region of noncollisional linear dissipation, at which point it cannot be treated by cascading mechanism. In the case of an electron Bernstein mode with perpendicular propagation linear dissipation is purely collisional while in the case of quasi-perpendicular propagation there exist regions on dispersion curves where noncollisional (Landau and cyclotron) dissipation is dominant [Ref. 23.b]. For other modes in ECFR such a noncollisional region always exists.

In order that collisional nonlinear dissipation be dominant, $N\omega_L$ is to be less than the hot-plasma dis persion correction of the corresponding modes. In the opposite case, a significant amount of energy is transferred into the noncollisional linear dissipation region and can lead to acceleration of electrons (tail plasma heating). In the upper limit of applicability of weak turbulence theory ($\gamma \sim \omega_L$) for bulk heating, through cascading processes, to be dominant γ^2/γ_H must be less than the hot-plasma dispersion correction of corresponding modes. In the case of excitation of upper-hybrid waves this condition gives:

$$\gamma^2 \lesssim \frac{1}{6}\gamma_{UH}\frac{\omega_{pe}^2}{\omega_{UH}}k_\perp^2\rho_e^2\,; \quad k_\perp^2\rho_e^2 < 1 \tag{45}$$

Note that in the case of very small k_d when $\omega_0 \sim \Omega_e(x)$ (which is realized in the vicinity of the line 1, Figure 3b) the low-frequency mode has a zero frequency and aperiodic instabilities can take place. In this case other saturation mechanisms are of interest (see for example Ref. 2 and Ref. 16). Decay instabilities and the cascading saturation mechanism take place in the shaded region (Figure 3.b) if inequality (45) is satisfied.

7. Comparison of Linear and Nonlinear Absorption Processes

In linear mode conversion theory of heating, the external power propagates freely toward the upper hybrid layer [Ref. 32] (see Figure 3.b) where it is linearly converted into a backward propagating electron Bernstein mode[33]; the electron Bernstein (EB) mode is then noncollisionally damped as it propagates into an electron cyclotron resonance region. However, if the energy level of EB mode is high, before it reaches the electron cyclotron resonance region it could be dissipated nonlinearly through cascading processes. Furthermore, if the turbulence level is very high $[(E_\ell^2)/(4\pi n_e \kappa T_e) \sim 1$ where E_ℓ^2 is the mean-square longitudinal mode electric field], which has been recently observed in simulation [Ref. 34], a strong coupling of excited modes occurs and the cascade turbulence spectrum is not discrete. Consequently, equation 2 is not valid and in the nonlinear treatment a ponderomotive force effect on the low-frequency mode must be taken into account. In addition, in this case electron trapping could also play a significant role as a saturation mechanism (in experiments and simulations it must lead to observation of suprathermal particles). This problem will be considered in a future paper.

In this paper we have been interested in parametric processes induced by the external pump. These appear possible in current experiments in tokamaks. Reactor type tokamaks are not likely to be parametrically heated unless high power gyrotrons ($I_0 \gtrsim 100\, kW/cm^2$) are constructed. However, regardless of the fact that the threshold values for reactor-type tokamak plasmas are high, nonlinear heating is of interest because it allows one to control the nonlinear dissipation rate (making it shorter than the confinement time) by changing the intensity of the external field. This is not possible in linear mode conversion heating where the dissipation rate depends on plasma parameters which are constant in a particular experiment.

Linear absorption lengths $\Delta x \sim 2R_0 n_\parallel (Te/m_e c^2)^{1/2}$ (R_0 is major radius, $n_\parallel = ck_\parallel/\omega$ parallel index of refraction) for $T_e \sim 1\, keV$, $R_0 \sim 100\, cm$ and $n_\parallel \sim 0.5$, amount to a value of several centimeters. The same values for the anomalous absorption lengths are also possible (in e.g.: $n_e \sim 10^{13}\, cm^{-3}$, $T_e \sim 1\, keV$, $B_0 \sim 5 - 10T$) if $I_0 \gtrsim 100\, kW/cm^2$. However for somewhat smaller temperatures $T_e \sim 200 - 500\, eV$, $R_0 \sim 50\, cm$, $n_e \sim 10^{12}\, cm^{-3}$ the required power flux is only of

the order of 1 kW/cm^2. Consequently, we can conclude that parametric processes can play a significant role and that saturation of these nonlinear excitations can involve cascadings. A verification of these processes would be the observation in experiments and/or simulations of discrete or semi-discrete turbulence spectra around a Stokes line.

REFERENCES

1. A. Bers, in Proc. of the Third Topical Conference on Radio Frequency Plasma Heating, Caltech (1978) pp. A1-1 – A1-10; V. V. Alikaev, Viniti, *Fizika Plazmi*, Vol. 2, Part 2, (1980), in Russian
2. M. Porkolab, R. P. H. Chang, *Reviews of Modern Physics*, Vol. 50, No. 4, October (1978).
3. V. A. Flyagin *et al., IEEE Trans. Microwave Theory Tech.*, 25, 514 (1977); J. L. Hirchfield and V. L. Granatstein, *IEEE Trans. Microwave Theory Tech.*, 25, 522 (1977).
4. V. V. Alikaev *et al., Fizika Plazmi*, 2, 390 (1976) [*Sov. J. Plasma Physics*, 2,212 (1976)]; R. M. Gilgenbach *et al., Phys. Rev. Letters* 44, 647 (1980). V. V. Alikaev *et al., Pis'ma Zh. Eksp. Teor. Fiz.* 35, No. 3, Feb. 1982 [*Sov. Phys. JETP Lett.*, Vol. 35, No. 3,5, Feb. 1982].
5. T. Cho *et al., Phys. Lett.* 77A, No. 5, 318 (1980).
6. T. M. Antonsen, Jr., M. Porkolab in *Physics of Plasma Close to Thermonuclear Conditions*, Vol. 1, CEC, Brussels (1980); T. M. Antonsen and W. M. Manheimer, *Phys. Fluids* 21, 2295, (1978).
7. E. Ott, B. Hui, K. R. Chu, *Phys. Fluids* 23, 5, May (1980).
8. G. Elder, F. W. Perkins, Jr., *IEEE Trans. on Plasma Science*, Vol. PS-8, No. 4, Dec. (1980).
9. V. Stefan, (a) 1st Joint Grenoble-Varenna Int. Symposium on Heating in Toroidal Plasmas, Grenoble (1978); (b) V. Stefan, 2nd Joint Grenoble-Varenna Int. Symposium on Heating in Toroidal Plasmas, Como (1980); (c) V. Stefan, *Phys. Lett. A* 32, 8 (1981).
10. R. A. Dandl *et al.*, in Proc. 6th Int. Conf. Plasma Phys. Contr. Nucl. Fusion Res., Berchtesgarden (1976), Vienna; EAEA, 1977, Vol. 1, 145.
11. S. Tanaka *et al., IEEE*, PS-8, No. 2, p. 68, June (1980).
12. R. P. H. Chang, M. Porkolab, B. Grek, *Phys. Rev. Lett.*, 28, 4,206 (1972); B. Grek. M. Porkolab, PPPL Report, Matt-S53 (1973).
13. V. Stefan, V. T. Tikhonchuk, *Phys. Rev. Lett.* 48, 21, 1476 (1982); V. Stefan, MIT Report, PFC/CP-82-3, March (1982).
14. A. G. Litvak *et al., Nucl. Fusion* 17, 4 (1977).
15. B. Hui *et al., Phys. Fluids* 23, 4 (1980).
16. V. P. Silin, *Parametric Action of a High Power Radiation on Plasma*, Moscow (1973), Chapt. 3, in Russian.
17. V. L. Ginzburg, A. A. Rukhadze, *Waves in Magnetized Plasma*, Nauka, Moscow (1975), in Russian, pp. 101-112.
18. B. D. Fried, S. Conte, *Plasma Dispersion Function*, Academic Press (1961).

19. L. V. Krupnova, V. T. Tikhonchuk, *JETP* 7, 1933 (1979); L. V. Krupnova, V. Stefan, V. T. Tikhonchuk, *Fizika Plazmi* 7, 6 (1981).

20. A. Bers, in *Handbook of Plasma Physics*, Vol. 1, Eds. A. A. Galeev, R. N. Sudan, North Holland Publishing Co., The Netherlands, 1983, Chapter 3.2, section 4.

21. See Ref. 20, section 5.

22. M. Tsutsui *et al., Phys. Lett.* 55A, 1, 31 (1975).

23. A. I. Akhiezer *et al., Plasma Electrodynamics*, Vol. 1, Pergamon Press, Oxford (1975); (a) pp. 354-358; (b) p. 269.

24. F. W. Chambers, A. Bers, *Phys. Fluids*, 20, 3, 466 (1977).

25. A. Bers, *Linear Waves and Instabilities*, in Plasma Physics – Les Houches, 1972; Gordon and Breach Publishers, 1975.

26. W. L. Kruer, E. J. Valeo, *Phys. Fluids* 16, 675 (1973).

27. A. A. Galeev, D. G. Lominadze, G. Z. Machabeli, *Sov. Phys. JTP 45*, 1938 (1975); S. Y. Yuen, *Phys. Fluids* 18, 1303 (1975).

28. V. Yu. Bychenkov, V. P. Silin, V. T. Tikhonchuk, *Sov. Phys. JETP Lett.* 26, 309 (1977).

29. V. F. Kovalyov and A. B. Romanov, *Sov. Phys. JETP* 7, 919 (1979).

30. R. R. Ramazasvilli and A. N. Starodub, *Fizika Plazmy* 6, 520 (1980) [*Sov. J. Plasma Physics* 6, 283 (1980)].

31. F. S. McDermott, G. Bekefi, K. E. Hackett, J. S. Levine, M. Porkolab, *Phys. Fluids Lett.*, Vol. 25, No. 9, 1488 (1982).

32. O. Eldrige, W. Namkung, A. C. England, ORNL/TM-6052, November (1977).

33. T. H. Stix, *Phys. Rev. Lett.* 15, 878 (1965).

34. A. T. Lin, Chin-Chien Lin and J. M. Dawson, *Phys. Fluids* 25(4), April 1982.

35. V. P. Silin and V. T. Tikhonchuk, *Phys. Lett. A*, 78, 246 (1980).

36. V. K. Tripathi and C. S. Liu, *Phys. Fluids*, Vol. 25, No. 8, 1388 (1982).

TABLE CAPTIONS

Table I. Linear dissipation rates for parametrically excited modes of interest are given. For high-frequency modes the relevant linear dissipation is collisional if $k_d \ll k_{coll}$. This is, however, always assumed in this paper as a crucial demand for the cascading saturation mechanism to be valid.

Table II. Decay wave numbers of primary excitations for parametric channels in ECFR. The decay wave number is a function of layer position in real space (Figure 3b), i.e., $k_d = \gamma[\omega_0 - \Omega_e(x)]$. Consequently, different layers will have different decay wave numbers. The cold and hot modes are defined by (37-40).

Table III. Anomalous absorption lengths for a variety of decay channels. The geometry employed in evaluating of quantities is as follows: $\vec{B}_0 = (0, 0, B_t)$; $\vec{k}_0 = (k_0, 0, 0)$ and $\vec{E}_0 = \{0, E_0, 0\}$. The wave vector of excited waves is in the (y, z) plane. κ is Boltzmann's constant. The values for ℓ_a are obtained utilizing expresions (43), (34) and (19).

TABLE I. LINEAR COLLISIONAL DISSIPATION OF EXCITED MODES

MODE	LINEAR DISSIPATION OF PARAMETRICALLY EXCITED MODES
Lower-Hybrid Wave	$\left(\frac{\gamma_{LH}}{\omega_{LH}}\right)_{coll} = \frac{\nu_{ei}}{2\omega_{LH}}\left(\frac{\omega_{LH}}{\omega^{LH}}\right)^2$
Upper-Hybrid Wave	$\left(\frac{\gamma_{UH}}{\omega_{UH}}\right)_{coll} = \frac{\nu_{ei}}{2\omega_{UH}}\left(1+\frac{\Omega_e^2}{\omega_{UH}^2}\right)$
Electron-Bernstein Wave	$\left(\frac{\gamma_{EB}}{\omega_{EB}}\right)_{coll} \sim \left(\frac{\gamma_{EB}}{\Omega_e}\right)_{coll} = \begin{cases} \frac{\nu_{ei}}{\Omega_e}\,;\ n=1 \\ \frac{\nu_{ei}}{\Omega_e}\frac{n^2+1}{2^n n!(n^2-1)^2}\frac{(k^2\rho_e^2)^{n+1}}{k^4 r_{De}^4}\,;\ n>1 \end{cases}$
Ion-Bernstein Wave	$\left(\frac{\gamma_{IB}}{\omega_{IB}}\right)_{coll} = \frac{5\nu_{ii}k^2\rho_i^2}{\omega_{IB}}\,,\ k^2\rho_i^2 \gg 1\,,\ \omega_{IB}\sim\Omega_i\,,\ n=1$ $\nu_{ei} \sim \left(\frac{m_i}{m_e}\right)^{1/2}\left(\frac{T_i}{T_e}\right)^{3/2}\nu_{ii}\,,\ \nu_{ei}\gg\nu_{ii}$
Ion-Acoustic Wave	$\frac{\gamma_s}{\omega_s} = \sqrt{\frac{\pi}{8}}\frac{m_i}{m_e}\frac{1}{z}\frac{\omega_s^3}{k^3 V_{Te}^3\lvert\cos\theta\rvert}\,,\ \theta = \sphericalangle(\vec{k}\,\vec{B})$ z – ion charge
Quasi Modes	$\frac{\gamma_{QM}}{\omega_{QM}} \to 1$

TABLE II. DECAY WAVE NUMBERS

The "cold" and "hot" modes are defined by expressions (37-40).

PRIMARY DECAY PROCESSES	DECAY WAVE NUMBER	
	"cold" modes	"hot" modes
$\omega_0 = \omega_{UH} + \omega_{LH}$	$\left(\frac{k_\parallel}{k}\right)_d^2 = \frac{2(\omega_0 - \omega_{UH})}{\omega_{LH}}\left(\frac{m_e}{m_i}\right)$	$k_d^2\rho_e^2 = \frac{2}{3}\frac{\omega_{LH}}{\Omega_e\Omega_i}\frac{T_e}{T_i}(\omega_0 - \omega_{UH})$
$\omega_0 = \omega_{EB} + \omega_s; \omega_{LH}; \omega_{IC}$	$k_d\rho_e = \left\{\frac{2\Omega_e(\omega_0 - \Omega_e)}{\omega_{pe}^2}\right\}^{1/2}$	$k_d\rho_e \ll 1\,,\ n = 1$
	$k_d\rho_e = \left\{2^n n!\frac{\omega_0 - n\Omega_e}{\omega_0}\frac{\Omega_e^2}{\omega_{pe}^2}\right\}^{\frac{1}{2(n-1)}}$	$n \neq 1$
$\omega_0 = \omega_{VH} + \omega_s$	$k_d = \frac{\omega_0 - \omega_{UH}}{V_s}\,,$	$V_s = \left(\frac{T_e}{m_i}\right)^{1/2}$

TABLE III. ANOMALOUS ABSORPTION LENGTHS (NORMAL INCIDENCE)

DRIVER PUMP FREQUENCY	DECAY WAVES	O-MODE	X-MODE
$\omega_0 = \omega_{EB} + \omega_{IS(H)}$ $\omega_{EB} = n\lvert\Omega_e\rvert\left\{1 + \frac{I_n(k^2\rho_i^2)}{k^2 r_{De}^2} e^{-k^2\rho_i^2}\right\}$ $\Omega_e \gtrsim \omega_{pe}$ $\omega_{IS(H)} = kV_s$	$EB + IS(H)$	Decay is not possible	$\ell_a = \frac{c}{2}\frac{4\Omega_e(4\pi n_e \kappa Te)^{1/2}}{(\Omega_e\omega_s)^{1/2}\omega_{pe}E_0}$, $n = 1$ $\ell_a = \frac{c}{2}\frac{4\Omega_e^3}{\omega_{pe}^3}\frac{2(n-1)(4\pi n_e\kappa T_e)^{1/2}}{(\Omega_e\omega_s)^{1/2}E_0}$, $n > 1$
$\omega_0 = \omega_{EB} + \omega_{IB}$ $\omega_{IB} = m\lvert\Omega_i\rvert\left\{1 + \frac{I_n(k^2\rho_i^2)}{k^2 r_{Di}^2} e^{-k^2\rho_i^2}\right\}$	$EB + IB$	Decay is not possible	$\ell_a = \frac{c}{2}\frac{2(k_d^2 r_{De}^2)^2\, k_d^2 r_{Di}^2\, \omega_{pi}\omega_{pe}\, 2^{\frac{m+n}{2}}(m!n!)^{1/2}}{\mu_n\, mn\, (\Omega_i\Omega_e)^{3/2}(k_d^2\rho_i^2)^{\frac{m+1}{2}}(k_d^2\rho_e^2)^{\frac{n+1}{2}}}$ $\mu_1^2 = \frac{k^2e^2E_0^2}{m_e^2\Omega_e^4}\left(\frac{\Omega_e}{\omega_{pe}}\right)^4$, $n = 1$; $\mu_n^2 = \mu_1^2\frac{\omega_{pe}^4}{\Omega e^4}\frac{1}{4(n-1)^2}$, $n > 1$
$\omega_0 = \omega_{EB} + \omega_{LH}$ $\omega_{LH} = \omega_{pi}\left(1 + \frac{\omega_{pe}^2}{\Omega_e^2}\right)^{-1/2}$	$EB + LH$	Decay is not possible	$\ell_a = \frac{c}{2}\frac{4\Omega_e}{(\omega_{LH}\Omega_e)^{1/2}\omega_{pe}k_d V_{De}}\frac{(4\pi n_e\kappa Te)^{1/2}}{E_0}$, $n = 1$ $\ell_a = \frac{c}{2}\frac{[8\cdot 2^n(n-1)!]^{1/2}\Omega_e k_d r_{De} 2(n-1)}{(\omega_{LH}\Omega_e)^{1/2}\omega_{pe}(k_d^2\rho_e^2)^{\frac{n+1}{2}}}\frac{(4\pi n_e\kappa Te)^{1/2}}{E_0}$, $n > 1$
$\omega_0 = \omega_{0EC} + \omega_{IS(H)}$ $\omega_{0EC} = \Omega_e\left\{1 + \frac{1}{2}\frac{\omega_{pe}^2}{\Omega_e^2}\sin^2\theta\right\}$	$OEC + IS(H)$	$\ell_a = \frac{c}{2}\frac{8\Omega_e^3}{\omega_{pe}^3}\frac{(4\pi n_e\kappa Te)^{1/2}}{\sin 2\theta(\Omega_e k_d V_s)^{1/2}E_0}$	$\ell_a = \frac{c}{2}\frac{4\Omega_e(4\pi n_e\kappa Te)^{1/2}}{(\Omega_e\omega_s)^{1/2}\omega_{pe}E_0}$
$\omega_0 = \omega_{0EC} + \omega_{IS(L)}$ $\omega_{IS(L)} = kV_s\cos\theta$	$OEC + IS(L)$	$\ell_a = \frac{c}{2}\frac{8\Omega_e^3}{\omega_{pe}^3}\frac{(4\pi n_e\kappa Te)^{1/2}}{(\Omega_e k_d V_s\cos\theta)^{1/2}(\cos\theta\sin 2\theta)E_0}$	$\ell_a = \frac{c}{2}\frac{4\Omega_e(4\pi n_e\kappa Te)^{1/2}}{\omega_{pe}(\Omega_e k_d V_s)^{1/2}(\cos^{3/2}\theta)E_0}$
$\omega_0 = \omega_{UH} + \omega_{IS(H)}$ $\omega_{UH} \sim (\omega_{pe}^2 + \Omega_e^2)^{1/2}$	$UH + IS(H)$	Decay is not possible	$\ell_a = \frac{c}{2}\frac{4k_d r_{De}}{\mu_x}\frac{\omega_{UH}}{\omega_{pe}(k_d V_s\omega_{UH})^{1/2}}$ $\mu_x = k_d r_{De}\frac{E_0}{(4\pi n_e\kappa Te)^{1/2}}$
$\omega_0 = \omega_{UH} + \omega_{LH}$ $\omega_{LH} = \omega_{pi}\left(1 + \frac{\omega_{pe}^2}{\Omega_e^2}\right)^{-1/2}$	$UH + LH$	Decay is not possible	$\ell_a = \frac{c}{2}\frac{4}{\mu_x}\frac{\omega_{UH}}{\omega_{pe}(\omega_{UH}\omega_{LH})^{1/2}}$

FIGURE CAPTIONS

Figure 1. Index of refraction $N = \frac{ck_0}{\omega_0}$ (k_0 is wavenumber of driver pump) for right-hand and left-hand polarized X-driver pump is shown for the case of strongly magnetized plasmas: $\Omega_e^2(x) \equiv (1+y)\omega_{pe}^2(x)$, where $0 \leq y \leq 1$. Here $\omega_L(x) = \frac{\omega_{pe}(x)}{2}(\sqrt{5+y} - \sqrt{1+y})$, $\omega_R(x) = \frac{\omega_{pe}(x)}{2}(\sqrt{5+y} - \sqrt{1+y})$ and $\omega_{UH}(x) = \omega_{pe}(x)\sqrt{2+y}$. ω_L denotes low-frequency parametrically excited waves. R_0 is the major radius of the torus.

Figure 2. Index of refraction for the O-mode. Other quantities are the same as in Figure 1.

Figure 3. Driver pump frequencies (X and O-mode) in terms of x (distance from the tokamak axis) are shown. On the cross section of (Figure 3.b) tokamak, a region of anomalous absorption of driver pump energy is shown. "A" denotes (Figure 3a) parametrically excited mode with local electron cyclotron frequency and "B" parametrically excited upper-hybrid wave. Anomalous absorption length is denoted by ℓ_a.

Figure 4. Dispersion curves for the harmonics of electron Bernstein modes. ($\Omega_e \gtrsim \omega_{pe}$). In the principal harmonic curve cascading processes always lead to the transfer of energy into short wave-length region (see arrows in points 1 and 2). Low-frequency parametrically excited mode is given by $\omega_{Ln} = \omega_0 - \Omega_e(x_n)$. Primary excitation in point 1 corresponds to the region around line 2 in Figure 3b, and in point 2 corresponds to the region around line 3 in Figure 3b. In the case of the second harmonic dispersion curve primary excitation in point 3 leads to the transfer of energy into the long wavelength region. Note that for modes shown linear dissipation is purely collisional.

NORMAL INCIDENCE

X-DRIVER PUMP

$$N^2 = 1 - \frac{\omega_{pe}^2}{\omega^2}\left[\frac{1-\omega_{pe}^2/\omega^2}{1-\omega_{UH}^2/\omega^2}\right]; \omega \sim \Omega_e$$

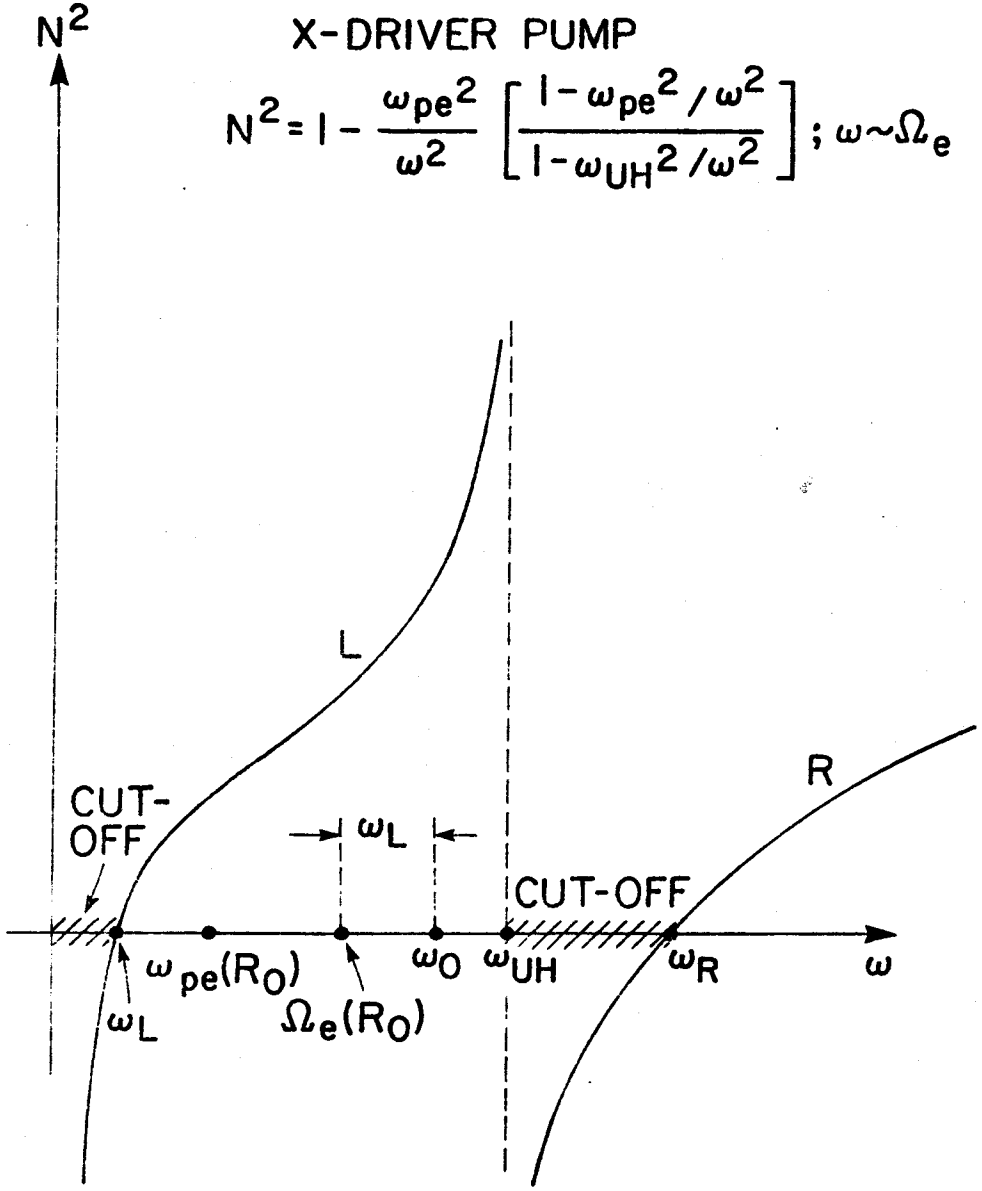

FIGURE 1

NORMAL INCIDENCE

O-DRIVER PUMP

$$N^2 = 1 - \frac{\omega_{pe}^2}{\omega^2}; \omega \sim \Omega_e$$

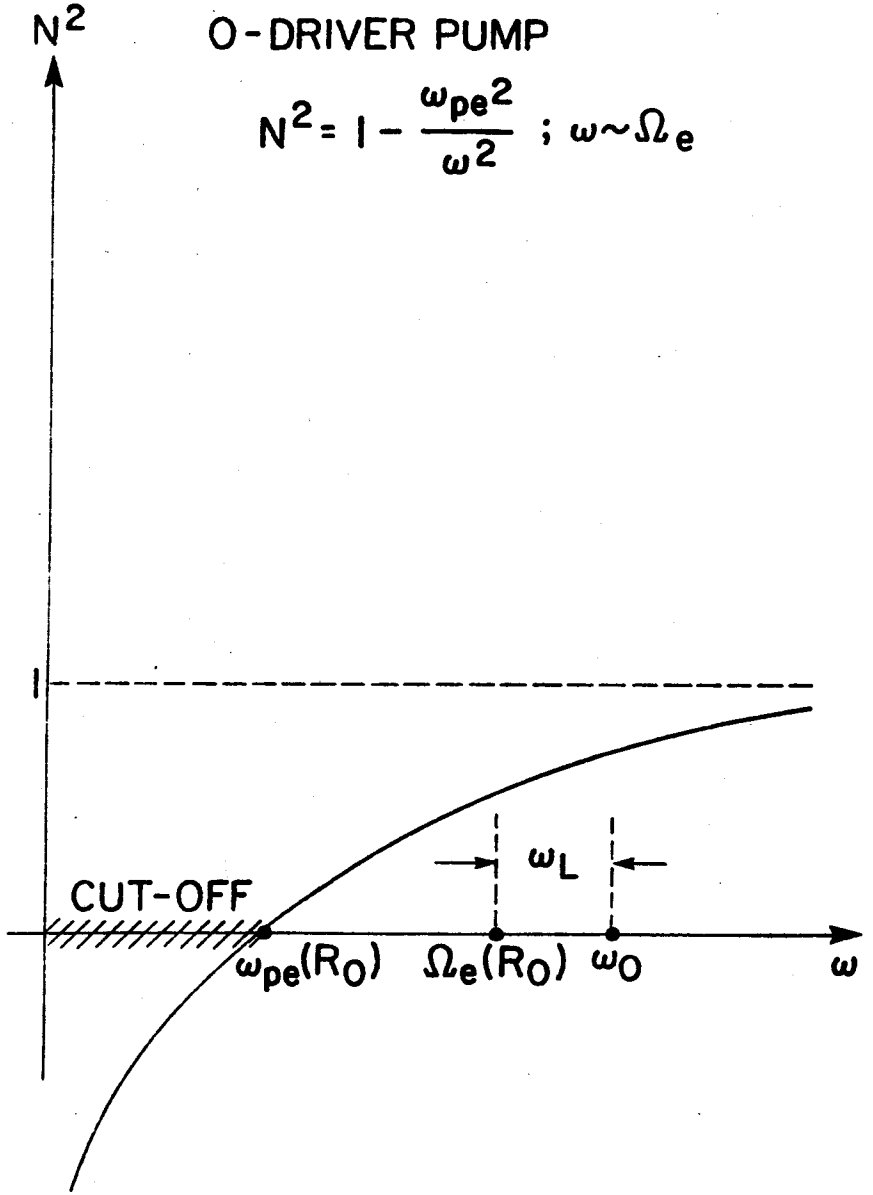

FIGURE 2

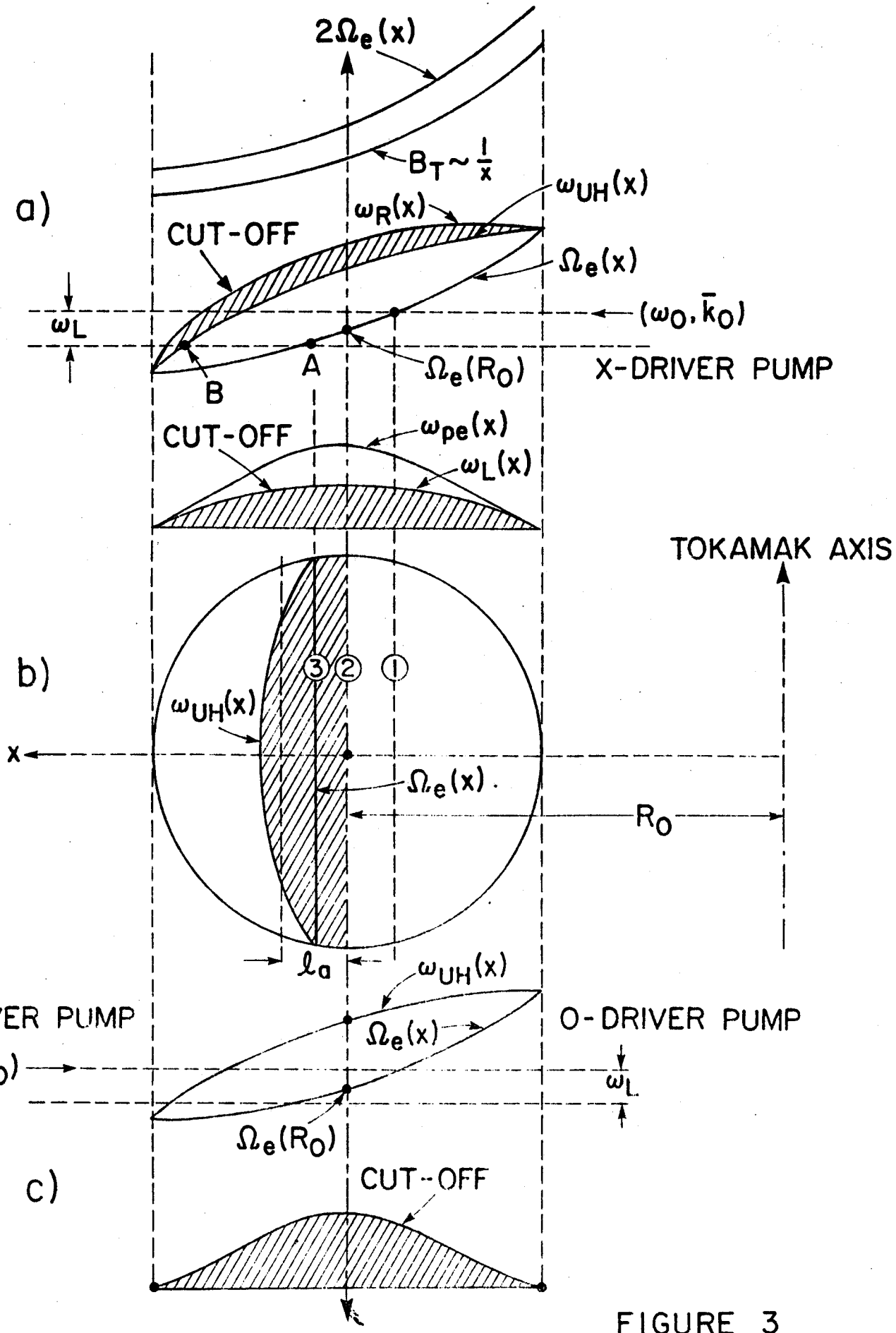
a)
$2\Omega_e(x)$
$B_T \sim \frac{1}{x}$
$\omega_{UH}(x)$
$\omega_R(x)$
CUT-OFF
$\Omega_e(x)$
$(\omega_0, \bar{k}_0)$
ω_L
A
B
$\Omega_e(R_0)$
X-DRIVER PUMP
CUT-OFF
$\omega_{pe}(x)$
$\omega_L(x)$
TOKAMAK AXIS
b)
3
2
1
$\omega_{UH}(x)$
x
$\Omega_e(x)$
R_0
l_a
$\omega_{UH}(x)$
O-DRIVER PUMP
O-DRIVER PUMP
$\Omega_e(x)$
$(\omega_0, \bar{k}_0)$
ω_L
$\Omega_e(R_0)$
c)
CUT-OFF

FIGURE 3

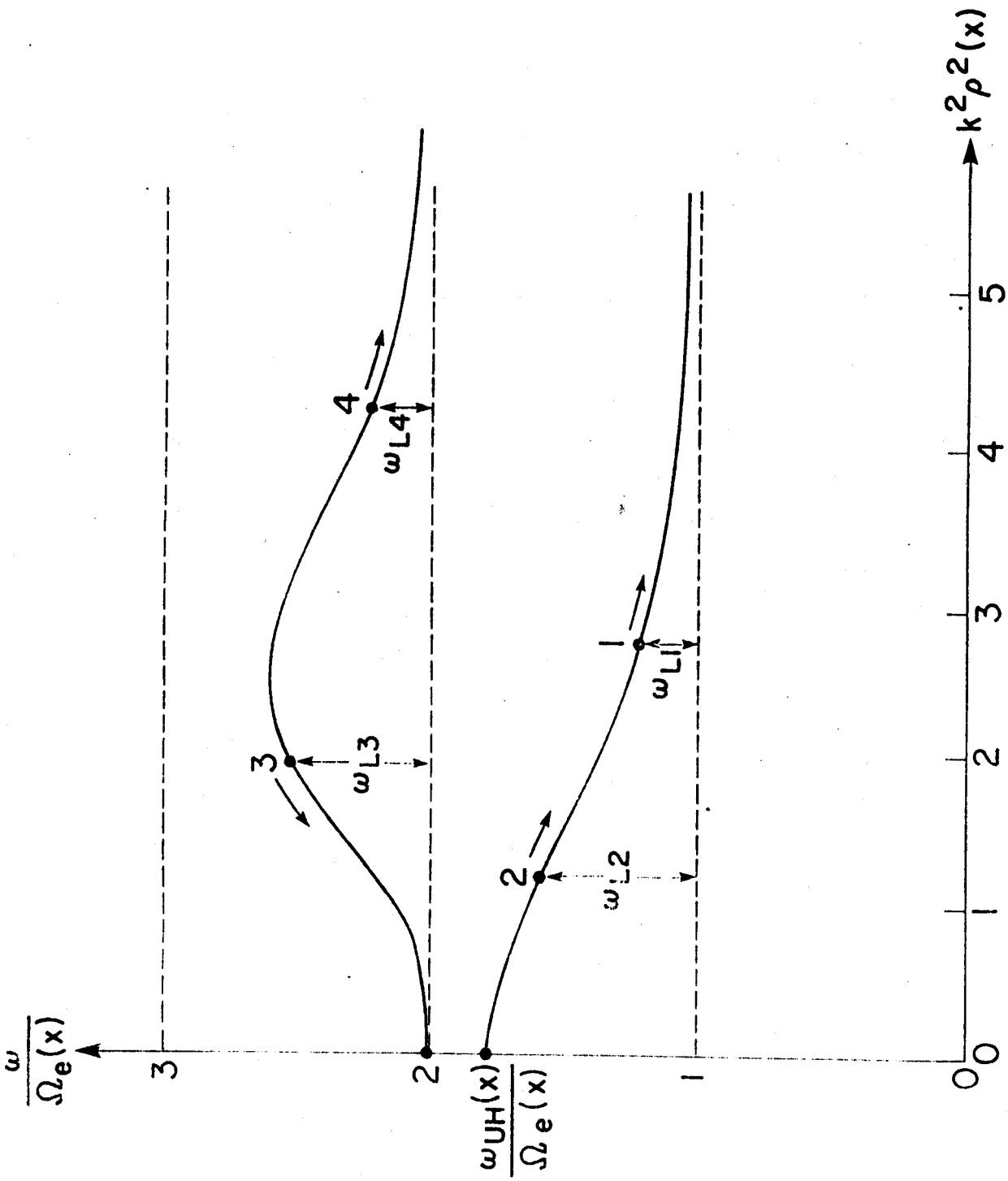
$\frac{\omega}{\Omega_e(x)}$
3
2
1
0
$\frac{\omega_{UH}(x)}{\Omega_e(x)}$
$k^2\rho^2(x)$
0
1
2
3
4
5
1
2
3
4
ω_{L1}
ω_{L2}
ω_{L3}
ω_{L4}

FIGURE 4